

Economic Optimization of Spray Dryer Operation using Nonlinear Model Predictive Control with State Estimation

Lars Norbert Petersen* John Bagterp Jørgensen**
James B. Rawlings***

* GEA Process Engineering A/S, Søborg, Denmark, (e-mail:
lars.n.petersen@gea.com)

** Department of Applied Mathematics and Computer Science,
Technical University of Denmark, Kgs. Lyngby, Denmark, (e-mail:
jbjo@dtu.dk)

*** Department of Chemical and Biological Engineering, University of
Wisconsin-Madison, Madison, USA, (e-mail: rawlings@engr.wisc.edu)

Abstract:

In this paper, we develop an economically optimizing Nonlinear Model Predictive Controller (E-NMPC) for a complete spray drying plant with multiple stages. In the E-NMPC the initial state is estimated by an extended Kalman Filter (EKF) with noise covariances estimated by an autocovariance least squares method (ALS). We present a model for the spray drying plant and use this model for simulation as well as for prediction in the E-NMPC. The open-loop optimal control problem in the E-NMPC is solved using the single-shooting method combined with a quasi-Newton Sequential Quadratic Programming (SQP) algorithm and the adjoint method for computation of gradients. We evaluate the economic performance when unmeasured disturbances are present. By simulation, we demonstrate that the E-NMPC improves the profit of spray drying by 17% compared to conventional PI control.

Keywords: Nonlinear Model Predictive Control, Optimization, Grey-box model, Spray Drying

1. INTRODUCTION

Spray drying is a processing technique for drying of liquids or slurries into a free flowing powder. Spray drying is a key process in the dairy industry (Mujumdar, 2006), where dairy products are dried into powders to increase the shelf life as well as to reduce cost of transportation over long distances. The quality of dairy powder is, among other factors, characterized by the residual moisture content that must be within the specification. Spray drying is by far the most energy-intensive unit operation in the dairy industry (IDF, 2005). Therefore, maximizing the efficiency of the spray drying process and maintaining the correct residual moisture level are of utmost importance.

The main challenge in controlling the spray dryer is to use a minimum of energy (hot air) to bring the residual moisture in the powder below the specification and to avoid that the powder sticks to the walls of the chamber. This is a challenge, as the operation of the spray dryer must continuously be adjusted to variations in the feed concentration and variations in the ambient air humidity. Application of advanced control is potentially a cost effective way to reduce the energy consumption as well as to increase the production capacity (Petersen et al., 2014b).

Conventional set-point based control of spray dryers keeps the inlet and outlet temperatures constant during operation. This approach is simple, but known to be insuffi-

cient for controlling the residual moisture. Furthermore, the powder may turn sticky inside the dryer during high ambient air humidities. This motivates E-NMPC in the presence of feed and ambient air variations. E-NMPC adjusts the manipulated variables in such a way that the residual moisture is below its maximum, fouling of the spray dryer is avoided, and the cost of operation is minimized.

1.1 Process Description

A Multi-Stage Dryer (MSDTM) consists of a spray chamber (SD), a static fluid bed (SFB), and two vibrating fluid bed (VFB) stages. This type of dryer is the most widely used dryer in the production of food powders (Mujumdar and Huang, 2007). Fig. 1 illustrates the stages of the spray dryer as well as the hot air and the powder in- and outlets. The dryer is designed such that the hot inlet air is fed into the upper section of the drying chamber around the high pressure nozzles. The nozzles disperse the liquid feed into droplets. The heat is transferred from the hot air to the droplets, which makes the water evaporate from the droplets. In that process, the air temperature and the residual moisture of the droplets decrease. The dried product then enters the SFB where it is further dried by hot air from below. Next, the powder is transported to the VFBh and VFBc stages for gentle drying and cooled to the temperature desired for handling and storage.

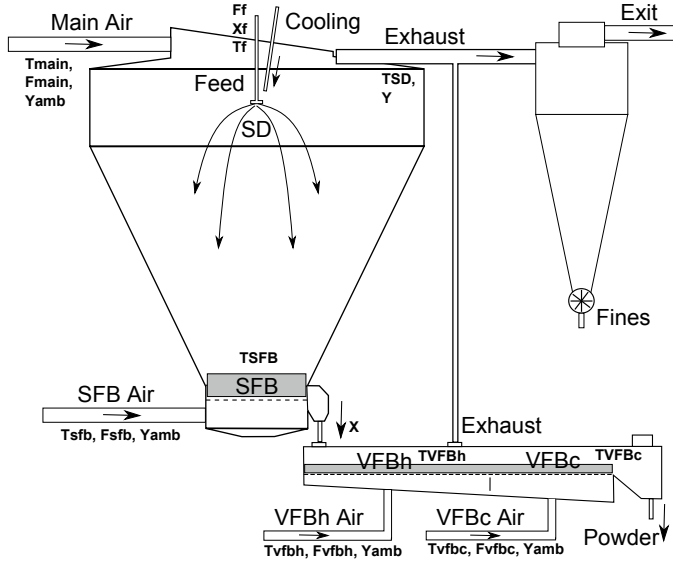


Fig. 1. Diagram of the spray dryer. Sprayed droplets and hot air are mixed in the top. The droplets dry into powder and are dried further in the SFB and VFBh stages and cooled in the VFBc stage.

1.2 Modeling

Dynamic models of spray drying has recently been reported. Petersen et al. (2013) propose a model for a complete spray dryer and Petersen et al. (2014a) presents a model for the SD and SFB stages of the spray dryer. The latter show good simulation accuracy. The model derived in this paper will therefore be based on the model in Petersen et al. (2014a) and extended to also describe the VFB stages.

1.3 Control and State Estimation

The combination of real-time steady-state optimization (RTO) and set-point based model predictive control is a standard methodology for optimizing process operation (Naysmith and Douglas, 1995). Recent advances within process optimization focus on optimizing the higher-level objectives, such as economics, directly in the control layer. This is called economically optimizing Model Predictive Control (E-MPC). For a long time, MPC has been the preferred advanced control methodology in the process industries. Recently, the idea of optimizing economics directly has gained significant renewed interest (Rawlings et al., 2012; Bauer and Craig, 2008). Papers related to control of spray dryers seldom consider an economic objective. Petersen et al. (2014a) discuss a linear tracking MPC, while Petersen et al. (2014b) discuss an E-NMPC for the SD and SFB stages of the spray dryer. Callaghan and Cunningham (2005) provides a thorough review on the status and future of advanced control for spray drying.

The model of the spray dryer is used for simulation as well as for prediction and state estimation in the NMPC. We use the well known extended continuous-discrete Kalman filter (EKF) for state estimation. The performance of the filter is highly dependent on good estimation of the noise covariances, which we will estimate using the Autocovariance Least-Squares (ALS) method described in Rajamani and Rawlings (2009).

1.4 Content & Organization

In this paper, we demonstrate that the profit of operation for a spray drying process can be improved significantly by application of E-NMPC based on an economically optimizing controller and an EKF for state estimation. The noise covariances in the EKF are estimated by the ALS method.

The paper is organized as follows. In Section 2, the model of the spray dryer is presented. Section 3 presents the estimation problem and the ALS method. Section 4 presents the control problem and its transcription to a computationally tractable optimization problem. In Section 5 we present a simulation to show the benefit of optimizing the operation. Conclusions are given in Section 6.

2. SPRAY DRYER MODEL

In this section, the complete spray dryer model is presented. It is derived from first engineering principles and describes drying of maltodextrin DE-18. We use Maltodextrin DE-18 as a substitute to milk, because milk is difficult to handle over longer periods due to natural deterioration.

2.1 Spray Dryer and Static Fluid Bed Model

The evolution of the temperatures, T_{SD} and T_{SFB} , is governed by energy balances, while mass balances determine the evolution of the air and powder moisture, Y_{ab} and X_{ab} . The lumped energy and mass balances describing the evolution of the states are

$$C_a \frac{dT_{SD}}{dt} = -\lambda R_{aw} + F_{main} h_{a_{in}} + F_{sfb} h_{b_{out}} - (F_{main} + F_{sfb} + F_{add}) h_{a_{out}} + F_{add} h_{a_{add}} + F_s (h_f^p - h_a^p) - Q_{ab} - Q_a \quad (1a)$$

$$C_b \frac{dT_{SFB}}{dt} = F_{sfb} (h_{b_{in}}^a - h_{b_{out}}^a) + F_s (h_a^p - h_b^p) + Q_{ab} - Q_{bc} - Q_b \quad (1b)$$

$$m_a \frac{dY_{ab}}{dt} = (F_{main} + F_{sfb})(Y_{amb} - Y_{ab}) + F_{add}(Y_{add} - Y_{ab}) + R_{aw} \quad (1c)$$

$$m_b \frac{dX_{ab}}{dt} = F_s (X_f - X_{ab}) - R_{aw} \quad (1d)$$

where

$$\begin{aligned} h_{a_{in}}^a &= (c_{da} + c_v Y_{amb}) T_{main}, & h_{a_{out}}^a &= (c_{da} + c_v Y_{ab}) T_{SD} \\ h_{b_{in}}^a &= (c_{da} + c_v Y_{amb}) T_{sfb}, & h_{b_{out}}^a &= (c_{da} + c_v Y_{amb}) T_{SFB} \\ h_{a_{add}}^a &= (c_{da} + c_v Y_{add}) T_{add}, & h_f^p &= (c_s + c_w X_f) T_f \\ h_a^p &= (c_s + c_w X_{ab}) T_{SD}, & h_b^p &= (c_s + c_w X_{ab}) T_{SFB} \\ Q_{ab} &= k_1 (T_{SD} - T_{SFB}) + k_2 X_f + k_3 T_f - k_4 \\ Q_a &= k_5 (T_{SD} - T_{amb}), & Q_b &= k_6 (T_{SFB} - T_{amb}) \end{aligned}$$

It is assumed that the air and the product are in equilibrium i.e. that the temperature of the air, T_{SD} and T_{SFB} , and the temperature of the product are identical. $h_{\{.\}}^a$ and $h_{\{.\}}^p$ are the specific enthalpies of the humid air and powder inlets and outlets of the SD and the SFB stages. C_a and C_b are the heat capacities of the hold-up of air and powder. The heat capacities are given at the reference temperature, $T_0 = 25^\circ\text{C}$. λR_{aw} is the heat of evaporation and Q_{ab} describes the heat exchange between the SD and

the SFB stages. F_{main} and F_{sfb} are the dry base inlet air flows. The parameters Y_{add} , F_{add} and T_{add} are used to compensate for air leakages and un-modeled inlet air flows such as nozzle cooling air. Q_a and Q_b are heat losses to the surroundings. $F_s = F_f X_f / (1 - X_f)$ is the flow of feed solids. X_f and T_f are the dry base feed concentration and feed temperature. m_a is the mass of dry air and m_b is the mass of dry powder.

We assume that the evaporation takes place in the SD stage only with the drying rate determined from conditions in the SFB. The product drying rate is governed by the thin layer equation, describing evaporation due to diffusion (Lewis, 1921)

$$R_{aw} = k_7 \frac{k_8}{k_8 + F_s} \left(\frac{T_f}{T_0} \right)^{k_9} (X_{ab} - X_{eq}(T_{\text{SFB}}, Y_{ab})) m_b$$

The equilibrium moisture content, $X_{eq}(T, Y)$, is a nonlinear product dependent function that describes the moisture content at which the water is bounded within the powder particles.

2.2 Vibrating Fluid Bed Model

The evolution of the temperatures, T_{VFBh} and T_{VFBc} , is governed by energy balances, while mass balances govern the evolution of the air humidity, Y_{cd} , and the moisture content, X_{cd} , in the powder.

$$C_{cd} \frac{dT_{\text{VFBh}}}{dt} = -\lambda R_{cw} + F_{\text{vfbh}}(h_{\text{cin}}^a - h_{\text{cout}}^a) + F_s(h_b^p - h_c^p) + Q_{bc} - Q_c \quad (2a)$$

$$C_{cd} \frac{dT_{\text{VFBc}}}{dt} = F_{\text{vfbh}}(h_{\text{din}}^a - h_{\text{dout}}^a) + F_s(h_c^p - h_d^p) - Q_d \quad (2b)$$

$$m_c \frac{dY_{cd}}{dt} = (F_{\text{vfbh}} + F_{\text{vfbh}})(Y_{\text{amb}} - Y_{cd}) + R_{cw} \quad (2c)$$

$$m_d \frac{dX_{cd}}{dt} = F_s(X_{ab} - X_{cd}) - R_{cw} \quad (2d)$$

where

$$\begin{aligned} h_{\text{cin}}^a &= (c_{da} + c_v Y_{\text{amb}}) T_{\text{vfbh}}, & h_{\text{cout}}^a &= (c_{da} + c_v Y_{cd}) T_{\text{VFBh}} \\ h_{\text{din}}^a &= (c_{da} + c_v Y_{\text{amb}}) T_{\text{vfbh}}, & h_{\text{dout}}^a &= (c_{da} + c_v Y_{cd}) T_{\text{VFBc}} \\ h_c^p &= (c_s + c_w X_{cd}) T_{\text{VFBh}}, & h_d^p &= (c_s + c_w X_{cd}) T_{\text{VFBc}} \\ Q_c &= k_{11}(T_{\text{VFBh}} - T_{\text{amb}}), & Q_d &= k_{12}(T_{\text{VFBc}} - T_{\text{amb}}) \\ Q_{bc} &= k_{10}(T_{\text{SFB}} - T_{\text{VFBh}}) \end{aligned}$$

$h_{\{\cdot\}}^a$ and $h_{\{\cdot\}}^p$ are the specific enthalpies of humid air and powder in and out of the VFBh and the VFBc stages. C_{cd} is the heat capacity of the hold-up of air and powder in each stage. m_c is the mass of dry air and m_d is the dry mass of powder. F_{vfbh} and F_{vfbh} are the dry base inlet and outlet air flows. Q_{bc} is the exchange of heat between the SFB and VFBh stage. Q_c and Q_d are heat losses to the surroundings. λR_{cw} is the heat of evaporation assumed to take place in the VFBh stage only. The product drying rate is governed from the thin layer equation and a constant term

$$R_{cw} = k_{13}(X_{cd} - X_{eq}(T_{\text{VFBh}}, Y_{cd})) m_d - k_{14} m_d$$

2.3 Stickiness

Stickiness of the produced particles is an important limitation to the achievable performance of the spray dryer.

Sticky particles form depositions on the walls of the spray dryer. Stickiness can be predicted by the glass transition temperature given by Boonyai et al. (2004)

$$T_g = \frac{T_{gp} + kZT_{gw}}{1 + kZ} \quad (3)$$

in which $T_{gp} = 144.8^\circ\text{C}$ (maltodextrin) and $T_{gw} = -137^\circ\text{C}$ (water). The value $k = 6.296$ is estimated from adsorption isotherm data. The obtained glass transition temperatures, T_g^{SD} and T_g^{SFB} , are the upper limiting temperatures of which deposits form on the chamber walls of the spray dryer. The moisture content of the powder is

$$Z = \begin{cases} (A_p + B_p T_{\text{SD}}) e^{C_p \text{RH}(T_{\text{SD}}, Y_{ab})} & \text{for SD} \\ X_{ab} & \text{for SFB} \\ X_{cd} & \text{for VFBh} \\ X_{cd} & \text{for VFBc} \end{cases}$$

in which $A_p = 0.193$, $B_p = -0.000435$ and $C_p = 4.51$. $\text{RH}(T_{SD}, Y_{ab})$ is the relative air humidity. The moisture content of the powder in the SD stage is difficult to estimate. Therefore, it is common practice to use an experimentally determined approximation related to the equilibrium moisture, $X_{eq}(T, Y)$.

2.4 Model

The model (1)-(3) of the dryer is a deterministic system of differential equations. In reality, the state and measurement equation of the dryer are corrupted by noise. Consequently, the deterministic system is augmented by two stochastic terms and we have a system of the form

$$x_{k+1} = F(x_k, u_k + w_{u,k}, d_k + w_{d,k}, \theta) \quad (4a)$$

$$y_k = h(x_k) + v_k \quad (4b)$$

The state and measurement noise covariances are $w_{u,k} = N_{iid}(0, T_s R_u)$, $w_{d,k} = N_{iid}(0, T_s R_d)$ and $v_k = N_{iid}(0, R_v)$. T_s is the sample time. The three noise-terms are assumed to be uncorrelated. $F(\cdot)$ is the state integration of $f(x_k, u_k, d_k, \theta)$ using a 3rd and 4th order accurate implicit Runge-Kutta (ESDIRK) method with variable step size (Kristensen et al., 2004). $h(\cdot)$ is the measurement equation.

The state vector, x , the manipulated input vector, u , and the disturbance vector, d are

$$x = \begin{bmatrix} T_{\text{SD}} \\ T_{\text{SFB}} \\ Y_{ab} \\ X_{ab} \\ T_{\text{VFBh}} \\ T_{\text{VFBc}} \\ Y_{cd} \\ X_{cd} \end{bmatrix} \quad u = \begin{bmatrix} F_f \\ T_{\text{main}} \\ T_{\text{sfb}} \\ T_{\text{vfbh}} \\ T_{\text{vfbh}} \end{bmatrix} \quad d = \begin{bmatrix} X_f \\ T_f \\ F_{\text{main}} \\ F_{\text{sfb}} \\ F_{\text{vfbh}} \\ F_{\text{vfbh}} \\ T_{\text{amb}} \\ Y_{\text{amb}} \end{bmatrix} \quad (5)$$

The measurement vector, y , is

$$y = [T_{\text{SD}} \ T_{\text{SFB}} \ Y_{ab} \ T_{\text{VFBh}} \ T_{\text{VFBc}} \ X_{cd}]^T \quad (6)$$

The noise variances, R_u , R_d and R_v , are based on manual inspection of the estimation data. The noise variances are unknown to the state estimator.

2.5 Parameter estimation

The parameters, θ , in the model (4) are estimated using data for a medium-scale spray dryer from GEA Process

Table 1. Estimated param. in model (1)-(3)

Sym.	Value	Unit	Sym.	Value	Unit
C_a	61.634	KJ/K	T_{add}	60.018	°C
C_b	148.26	KJ/K	k_7	$9.401 \cdot 10^{-2}$	-
k_1	0.2725	KW/K	k_8	$1.4887 \cdot 10^{-2}$	-
k_2	1.5017	KW	k_9	8.4203	-
k_3	0.0605	KW/K	C_{cd}	29.244	KW/K
k_4	27.276	KW	k_{10}	$9.561 \cdot 10^{-3}$	KW/K
k_5	0.24735	KW/K	k_{11}	$22.314 \cdot 10^{-3}$	KW/K
k_6	-0.03198	KW/K	k_{12}	$46.818 \cdot 10^{-3}$	KW/K
F_{add}	248.54	kg/hr	k_{13}	$1.9963 \cdot 10^{-3}$	-
Y_{add}	9.4566	g/kg	k_{14}	$13.49 \cdot 10^{-6}$	-

Engineering A/S. Table 1 provides the least squares estimated parameters of the model. $m_a = 7.5$ kg, $m_b = 15$ kg, $m_c = 15$ kg and $m_d = 4$ kg are fixed parameters and determined from physical considerations. Generally the model fits and predicts the data well both for the estimation and validation data, respectively.

2.6 Constraints

The maximum capacity of the feed pump limits the feed flow such that $0 \text{ kg/hr} \leq F_f \leq 130 \text{ kg/hr}$. The inlet temperatures must be higher than the ambient temperature, T_{amb} , as the dryer can only heat and not cool the air. Furthermore, the risk of powder explosions and the risk of scorched particles creates upper limits on the allowable inlet temperatures. Consequently, $T_{amb} \leq T_{main} \leq 200^\circ\text{C}$, $T_{amb} \leq T_{sfb} \leq 120^\circ\text{C}$, $T_{amb} \leq T_{vfbh} \leq 80^\circ\text{C}$ and $T_{amb} \leq T_{vfbc} \leq 80^\circ\text{C}$. These constraints are hard input constraints of the form (9d).

To avoid depositions of sticky particles on the spray dryer surfaces, the temperatures T_{SD} , T_{SFB} , T_{VFBh} and T_{VFBc} must be below the glass transition temperatures in the SD stage, $T_{SD} \leq T_g^{SD}$, the SFB stage, $T_{SFB} \leq T_g^{SFB}$, the VFBh stage, $T_{VFBh} \leq T_g^{VFBh}$ and the VFBc stage, $T_{VFBc} \leq T_g^{VFBc} \leq 35^\circ\text{C}$, respectively. The glass transition temperatures are determined by (3). Furthermore, the powder moisture must be below a maximum limit, $X_{cd} \leq X_{max} = 3.5\%$, that is 3.5% for the case study in this paper. These constraints are treated as soft output constraints in the form (10e). The soft ℓ_1 penalty is $s_W = 10^4 \cdot T_s \cdot [1 \ 1 \ 1 \ 1 \ 0.1]$ and the soft ℓ_2 penalty is $S_W = \text{diag}(s_W)$.

2.7 Key Performance Indicators (KPIs)

The profit from operating the spray dryer is the value of the product minus the raw material and energy costs

$$p(x(t), u(t), d(t)) = p_p F_s(1 + X_{cd}) - p_f F_s(1 + X_f) - p_H \Delta H \quad (7)$$

in which p_p is the unit value of the product, p_f is the unit cost of feed material, p_H is the unit energy cost, and ΔH is the total energy supplied to the dryer. ΔH is

$$\Delta H = F_{main}(h_{a_{in}}^a - h_{amb}^a) + F_{sfb}(h_{b_{in}}^a - h_{amb}^a) + F_{vfbh}(h_{c_{in}}^a - h_{amb}^a) + F_{vfbc}(h_{d_{in}}^a - h_{amb}^a)$$

in which $h_{amb}^a = (c_{da} + c_v Y_{amb})T_{amb}$. The price of, the produced powder is $p_p = 4.47$ \$/kg, the feed material is $p_f = 0.447$ \$/kg, and the energy is $p_H = 34.873$ \$/GJ. The prices are selected to reflect industrial reality meaning that

the price of natural gas is almost negligible compared to the price of the powder, i.e. $p_p \gg p_H$.

The energy efficiency of operation and the product flow rate are also key performance indicators for evaluation of the performance of a spray dryer. The energy efficiency is

$$\eta = \frac{\lambda F_s(X_f - X_{cd})}{\Delta H}$$

Here $\lambda F_s(X_f - X_{cd})$ is the energy used to evaporate water and ΔH is the total energy supplied. The flow rate of the produced powder is

$$F_p = F_s(1 + X_{cd})$$

3. STATE ESTIMATION PROBLEM

In the following, we will use an extended Kalman Filter (EKF), consisting of a filtering part and a one-step predictor part, to estimate the states of the nonlinear stochastic system described in (4).

3.1 Offset-free output estimation

The regulator and state estimator are based on the augmented model in order to achieve offset-free output estimation at steady-state, in the presence of plant/model mismatch and/or un-modeled disturbances (Pannocchia and Rawlings, 2003). We define the augmented model as

$$\bar{x}_{k+1} = \bar{F}(\bar{x}_k, u_k, \bar{d}_k, \bar{\theta}) + \bar{w}_k \quad (8a)$$

$$\bar{y}_k = \bar{h}(\bar{x}_k) + \bar{v}_k \quad (8b)$$

in which \bar{F} is the time integral of \bar{f} and \bar{h} is the output equation. $\bar{x}(t_k)$ is the estimated state, \bar{d} is the measured disturbances and $\bar{\theta}$ is the model parameters that both may differ from the true value in (4). The state and measurement noise covariances are $\bar{w}_k = N_{iid}(0, \bar{R}_w)$ and $\bar{v}_k = N_{iid}(0, \bar{R}_v)$ and estimated in Sec. 3.3 from data. We select pure input disturbances such that the energy- and the vapor mass balances are subject to the disturbance integration.

3.2 State estimator

The EKF utilizes many of the same principles as the Kalman filter. However it linearizes the non-linear model around the current estimate at each time step allowing the system to be solved as a linear time varying (LTV) system.

The estimator consists of a filtering part and a one-step predictor part. The filtering part corrects $\hat{x}_{k|k}$, using the latest measurement, y_k . $\hat{x}_{k|k}$ is used in the controller as the initial state. The predictor part uses the model to predict $\hat{x}_{k+1|k}$. Assuming that the state and measurement noise are uncorrelated, we get the filter equations

$$\hat{x}_{k|k} = \hat{x}_{k|k-1} + K_{f,x,k}(y_k - \bar{h}(\hat{x}_{k|k-1}))$$

$$P_{k|k} = P_{k|k-1} - K_{f,x,k} R_{e,k} K_{f,x,k}^T$$

where the Kalman gains are

$$R_{e,k} = C_k P_{k|k-1} C_k^T + \bar{R}_v$$

$$K_{f,x,k} = P_{k|k-1} C_k^T R_{e,k}^{-1}$$

The one-step predictor is

$$[\hat{x}_{k+1|k}, S_{x,k}] = \text{ESDIRK}(\hat{x}_{k|k-1}, u_k, \bar{d}_k, \bar{\theta})$$

$$P_{k+1|k} = S_{x,k} P_{k|k} S_{x,k}^T + G \bar{R}_w G^T$$

In the above we have $C_k = \frac{d\bar{h}}{d\bar{x}} \Big|_{\hat{x}_{k|k-1}}$ and $G = I$. The state estimator needs a good estimate of the process and measurement noise covariances to work properly. To achieve this we will use the ALS method.

3.3 ALS Estimator tuning

Rajamani and Rawlings (2009) describes a method for estimating the noise covariances based on data, the LTI discrete-time model of the augmented system and an initial guess on the noise sources. We obtain the LTI discrete-time model by linearization and discretization of (8). The estimate of the states are then constructed by the stationary Kalman filter as

$$\hat{x}_{k+1} = \bar{A}\hat{x}_{k|k-1} + \bar{B}u_k + \bar{E}d_k + \bar{A}L(y_k - \bar{C}\hat{x}_{k|k-1})$$

The state estimation error then evolves as

$$\epsilon_{k+1} = (\bar{A} - \bar{A}L\bar{C})\epsilon_k + [I - \bar{A}L] \begin{bmatrix} \bar{w}_k \\ \bar{v}_k \end{bmatrix}$$

In which \bar{A} , \bar{B} , \bar{E} and \bar{C} are the state, input, disturbance and output LTI system matrices of (8). L is the static Kalman gain constructed from the initial guess of the noise sources and the LTI model. (\bar{A}, \bar{C}) is detectable and $\bar{A} - \bar{A}L\bar{C}$ is stable. The innovations, \mathcal{Y}_k , are constructed by

$$\mathcal{Y}_k = \bar{C}\epsilon_k + v_k$$

and the auto covariance is constructed by $E(\mathcal{Y}_k \mathcal{Y}_{k+1}^T)$. From \mathcal{Y}_k , ϵ_{k+1} and the LTI model we can construct a constrained ALS estimation problem, that enforces positive semi-definiteness, to estimate the noise variances by

$$\begin{aligned} \Phi &= \min_{\bar{R}_w, \bar{R}_v} \left\| \mathcal{A} \begin{bmatrix} (\bar{R}_w)_s \\ (\bar{R}_v)_s \end{bmatrix} - \hat{b} \right\|_2^2 + \rho \text{tr}(\bar{R}_w) \\ \text{s.t.} \quad &\bar{R}_w \geq 0, \bar{R}_v \geq 0 \end{aligned}$$

in which \mathcal{A} and \hat{b} are constructed according to Rajamani and Rawlings (2009). The problem is convex and can be solved efficiently even for large datasets. We select the initial state noise covariance $\bar{R}_w = I \cdot 10^{-3}$ and measurement noise $\bar{R}_v = I \cdot 10^{-4}$. The data set used for the estimation is made from an open loop simulation of the nonlinear system with step disturbances in X_f , T_f and Y_{amb} . It contains 650 data points of which the first 10 points are for initialization of the Kalman Filter. The estimated \bar{R}_w and \bar{R}_v in combination with the disturbance structure render a satisfactory performance in the EKF and provides offset-free output estimation.

4. OPTIMAL CONTROL PROBLEM

In this section, we present the continuous-time constrained optimal control problem and its transcription to a discrete time optimal control problem. We solve the discrete optimal control problem using the single-shooting method.

4.1 Continuous-Time Const. Optimal Control Problem

In a receding horizon manner, the manipulated variables in the E-NMPC considered in this paper are obtained by

the solution of the following continuous-time constrained optimal control problem in Lagrange form

$$\min_{\bar{x}(\cdot), u(\cdot), s(\cdot)} \phi = \int_{t_0}^{t_f} [-p(\bar{x}(t), u(t), \bar{d}(t)) + \phi(s(t))] dt \quad (9a)$$

$$\text{s.t.} \quad \bar{x}(t_0) = \hat{x}_0, \quad (9b)$$

$$\frac{d\bar{x}(t)}{dt} = \bar{f}(\bar{x}(t), u(t), \bar{d}(t), \bar{\theta}), \quad t \in \mathcal{T} \quad (9c)$$

$$u_{\min} \leq u(t) \leq u_{\max}, \quad t \in \mathcal{T} \quad (9d)$$

$$c(\bar{x}(t)) + s(t) \geq 0, \quad t \in \mathcal{T} \quad (9e)$$

$$s(t) \geq 0, \quad t \in \mathcal{T} \quad (9f)$$

in which $\mathcal{T} = [t_0, t_f]$. $\bar{x}(t) \in \mathbb{R}^{n_x}$ is the state vector, $u(t) \in \mathbb{R}^{n_u}$ is the manipulated variables, $\bar{d}(t) \in \mathbb{R}^{n_d}$ is the known disturbance vector, and $s(t) \in \mathbb{R}^{n_s}$ are the slack variables related to the soft output constraints. The initial state $\bar{x}(t_0) = \hat{x}_0$ and the period $[t_0, t_f]$ are fixed. At each sample time t_0 is the current time and t_f is the prediction and control horizon. The current state, \hat{x}_0 , is assigned to the initial state by (9b). The stage cost function, $-p(\bar{x}(t), u(t), \bar{d}(t))$, represents the cost of operation, (9c) represents the process dynamics, and (9d) is hard input constraints. $\phi(s(t)) = \frac{1}{2} \|s(t)\|_{2, SW}^2 + \|s(t)\|_{1, SW}$ and (9e)-(9f) represent $\ell_2 - \ell_1$ soft output constraints.

4.2 Transcription

The infinite-dimensional optimal control problem (9) is converted to a numerically tractable finite-dimensional optimal control problem by 1) parametrization of the control vector, $u(t)$, and the disturbance vector, $\bar{d}(t)$, 2) point-wise Dirac delta approximation of the soft output constraints, and 3) discretization of the dynamics (9c) and the objective integral. Using these approximations, (9) may be transcribed into the finite dimensional discrete optimal control problem

$$\min_{\bar{x}, u, s} \phi = \sum_{k=0}^{N-1} [-P_k(\bar{x}_k, u_k, \bar{d}_k) + \phi(s_k)] + \phi_{\Delta u} \quad (10a)$$

$$\text{s.t.} \quad \bar{x}_0 = \hat{x}_0, \quad (10b)$$

$$R_k(\bar{x}_k, \bar{x}_{k+1}, u_k, \bar{d}_k, \bar{\theta}) = 0, \quad k \in \mathcal{N} \quad (10c)$$

$$u_{\min} \leq u_k \leq u_{\max}, \quad k \in \mathcal{N} \quad (10d)$$

$$c(\bar{x}_k) + s_k \geq 0, \quad k \in \mathcal{N} \quad (10e)$$

$$s_k \geq 0, \quad k \in \mathcal{N} \quad (10f)$$

with $\mathcal{N} = \{0, 1, \dots, N-1\}$ and N being the discrete prediction and control horizon. The discrete stage cost, $P_k(\bar{x}_k, u_k, \bar{d}_k)$, and the residual function, $R_k = R_k(\bar{x}_k, \bar{x}_{k+1}, u_k, \bar{d}_k, \bar{\theta}) = \bar{x}_{k+1} - \bar{F}(\bar{x}_k, u_k, \bar{d}_k, \bar{\theta})$, are obtained using the ESDIRK3(4) method. The ESDIRK integration method and the computation of the state and stage cost sensitivities are described in Kristensen et al. (2004); Capolei and Jørgensen (2012). The scheme has been implemented with fixed step size using 5 intermediate steps. No forecasts are available for the disturbances, so we use the same-as-now forecasts, i.e. $\bar{d}_k = \bar{d}(t_0)$.

In order to obtain smooth solutions we add the regularization term that penalizes changes in the manipulated variables

$$\phi_{\Delta u} = \sum_{k=0}^{N-1} \|u_k - u_{k-1}\|_{Q_s}^2$$

We use $Q_s = T_s \cdot \text{diag}([0.5; 1; 0.5; 0.5; 0.5])$.

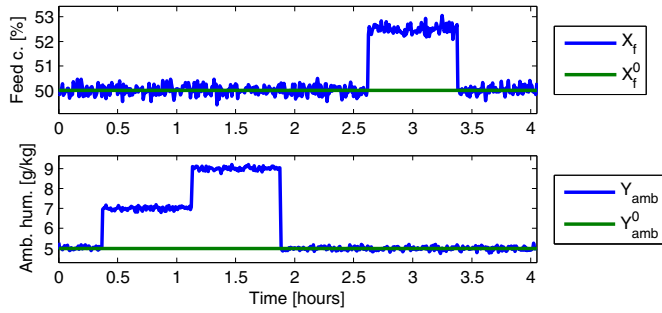


Fig. 2. Disturbance scenario for the case studies.

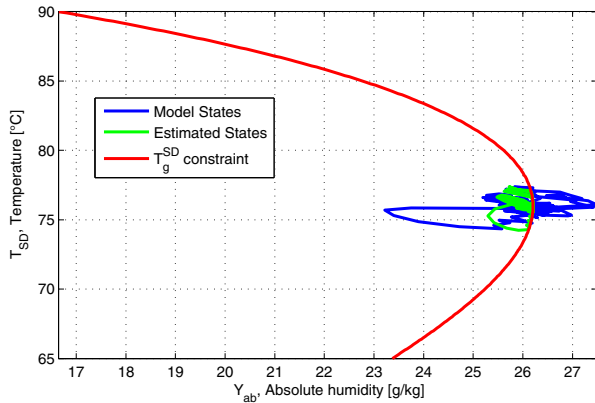


Fig. 3. Active inequality constraint from (3) that constrains T_{SD} and Y_{ab} . Notice, that cost optimal operation is achieved by maximizing Y_{ab} within the non-sticky region.

4.3 Single-Shooting Optimization

In this paper, the optimal control problem (10) is solved by the single-shooting method using a quasi-Newton SQP optimization algorithm (`fmincon` in Matlab's optimization toolbox) and the adjoint method for gradient computation (Petersen and Jørgensen, 2014). The sample time is chosen as $T_s = 30$ s and we use a control and prediction horizon of $t_f = 35$ min i.e. $N = 70$.

5. RESULTS

We illustrate the performance of the E-NMPC by a closed-loop simulation.

5.1 Simulation

Fig. 2 illustrates the feed concentration and the ambient air humidity disturbances considered in the simulated scenario. These renders maximum day-to-day variations.

Fig. 4 shows E-NMPC closed-loop response operation of the spray dryer. Fig. 4(a) shows the outputs and Fig. 4(b) shows the manipulated variables. Fig. 4(c) illustrates the energy efficiency, the production rate and the operational profit rate. Note that the operational profit rate is largely dictated by the production rate. The E-NMPC pushes the system to the constraints in order to maximize profit. In this example, the active constraints are the stickiness

constraint in the SD stage, T_g^{SD} , and the maximum allowed residual moisture content in the powder, X_{max} . An increase in ambient air humidity, Y_{amb} , decreases the evaporation rate, R_w , of the dryer and the powder becomes more moist and sticky. The E-NMPC compensates by decreasing the production rate i.e. it decreases the feed rate, F_f , and the inlet air temperatures. A step increase in the feed (water) concentration, X_f , increases the amount of water that has to be evaporated from the feed. The E-NMPC compensates again by decreasing the production rate. Consequently, the economically most favorable conditions for the dryer is obtained at low ambient air humidity and feeds with a high solids content. The sticky temperature, T_g^{SD} in (3), is only a function of the states Y_{ab} and T_{SD} . Thus, we can plot this constrain in 2D. Fig. 3 illustrates T_g^{SD} and shows that one can form a sticky and non-sticky region where cost optimal operation is achieved by maximizing Y_{ab} within the given non-sticky region. The stickiness constraint, T_g^{SD} , and the residual moisture content, X_{cd} , violates the constraints slightly. A back-off strategy must therefore be implemented to avoid constraint violation at any time.

Cost optimal operation of the plant is not guaranteed to be obtained in general by model based optimization due to plant and model mismatch as well as the presence of unknown disturbances. We obtain almost exact cost optimal plant operation for the disturbance scenario in Fig. 2. This is primarily due to the definition of the active constraints, that do not depend on the unknown disturbances, but only on the measured states T_{SD} , Y_{ab} and X_{cd} .

As illustrated in Fig. 4(c), the profit of operation depends mainly on the production rate, the feed concentration and the residual moisture of the final powder. The energy usage is a secondary objective. Fortunately, the energy efficiency is maximized for a given production rate, but higher efficiencies can be achieved at the sacrifice of production capacity. The PI controller controls the temperature T_{SD} by manipulating the feed flow F_f . Thus, it does not perform any correcting action to compensate for changes in the ambient air humidity. A considerably back-off from the stickiness constraint must therefore be enforced leading to reduced production and profit loss. On average, for the given disturbance scenario, the E-NMPC increases the profit of operation by 17% compared to the conventional PI controller.

6. CONCLUSIONS

This paper presents an economically optimizing control solution for a spray dryer. The E-NMPC provides a control solution that constantly brings the dryer to the most cost optimal state of operation. The residual moisture is controlled within specifications and deposition of sticky particles on spray dryer surfaces are avoided. This is achieved by the ability of the E-NMPC to include stickiness constraints and compute control profiles that are continuously adapted to variations in the feed and the ambient conditions. On average, for the given disturbance scenario, the E-NMPC increases the profit of operation by 17% compared to the conventional PI controller.

REFERENCES

- Bauer, M. and Craig, I.K. (2008). Economic assessment of advanced process control – a survey and framework. *Journal of Process Control*, 18(1), 2–18.
- Boonyai, P., Bhandari, B., and Howes, T. (2004). Stickiness measurement techniques for food powders: a review. *Powder Technology*, 145(1), 34–46.
- Callaghan, D.O. and Cunningham, P. (2005). Modern process control techniques in the production of dried milk products – a review. *Lait*, 85, 335–342.
- Capolei, A. and Jørgensen, J.B. (2012). Solution of constrained optimal control problems using multiple shooting and esdirk methods. *Proceedings of the 2012 American Control Conference*, 295–300.
- IDF (2005). Energy use in dairy processing. in: Bulletin of the international dairy federation. *International Dairy Federation*, 401.
- Kristensen, M.R., Jørgensen, J.B., Thomsen, P.G., and Jørgensen, S.B. (2004). An ESDIRK method with sensitivity analysis capabilities. *Computers & Chemical Engineering*, 28(12), 2695–2707.
- Lewis, W.K. (1921). The rate of drying of solid materials. *Journal of Industrial and Engineering Chemistry*, 13, 427–432.
- Mujumdar, A.S. and Huang, L.X. (2007). Global R&D needs in drying. *Drying Technology*, 25(4), 647–658.
- Mujumdar, A.S. (2006). *Handbook of Industrial Drying, Third Edition*. CRC Press, Boca Raton, FL.
- Naysmith, M.R. and Douglas, P.L. (1995). Review of real time optimization in the chemical process industries. *Developments in Chemical Engineering and Mineral Processing*, 67–87.
- Pannocchia, G. and Rawlings, J.B. (2003). Disturbance models for offset-free model-predictive control. *AIChE Journal*, 49(2), 426–437.
- Petersen, L.N. and Jørgensen, J.B. (2014). Real-time economic optimization for a fermentation process using model predictive control. *13th European Control Conference*.
- Petersen, L.N., Poulsen, N.K., Niemann, H.H., Utzen, C., and Jørgensen, J.B. (2013). A Grey-Box Model for Spray Drying Plants. *10th IFAC International Symposium on Dynamics and Control of Process Systems*, 559–564.
- Petersen, L.N., Poulsen, N.K., Niemann, H.H., Utzen, C., and Jørgensen, J.B. (2014a). Application of constrained linear mpc to a spray dryer. *Proceedings of the IEEE Multi-Conference on Systems and Control*.
- Petersen, L.N., Poulsen, N.K., Niemann, H.H., Utzen, C., and Jørgensen, J.B. (2014b). Economic optimization of spray dryer operation using nonlinear model predictive control. *Proceedings of the IEEE Conference on Decision and Control*.
- Rajamani, M.R. and Rawlings, J.B. (2009). Estimation of the disturbance structure from data using semidefinite programming and optimal weighting. *Automatica*, 45(1), 142–148.
- Rawlings, J.B., Bates, C.N., and Angeli, D. (2012). Fundamentals of economic model predictive control. *Proceedings of the IEEE Conference on Decision and Control*, 3851–3861.

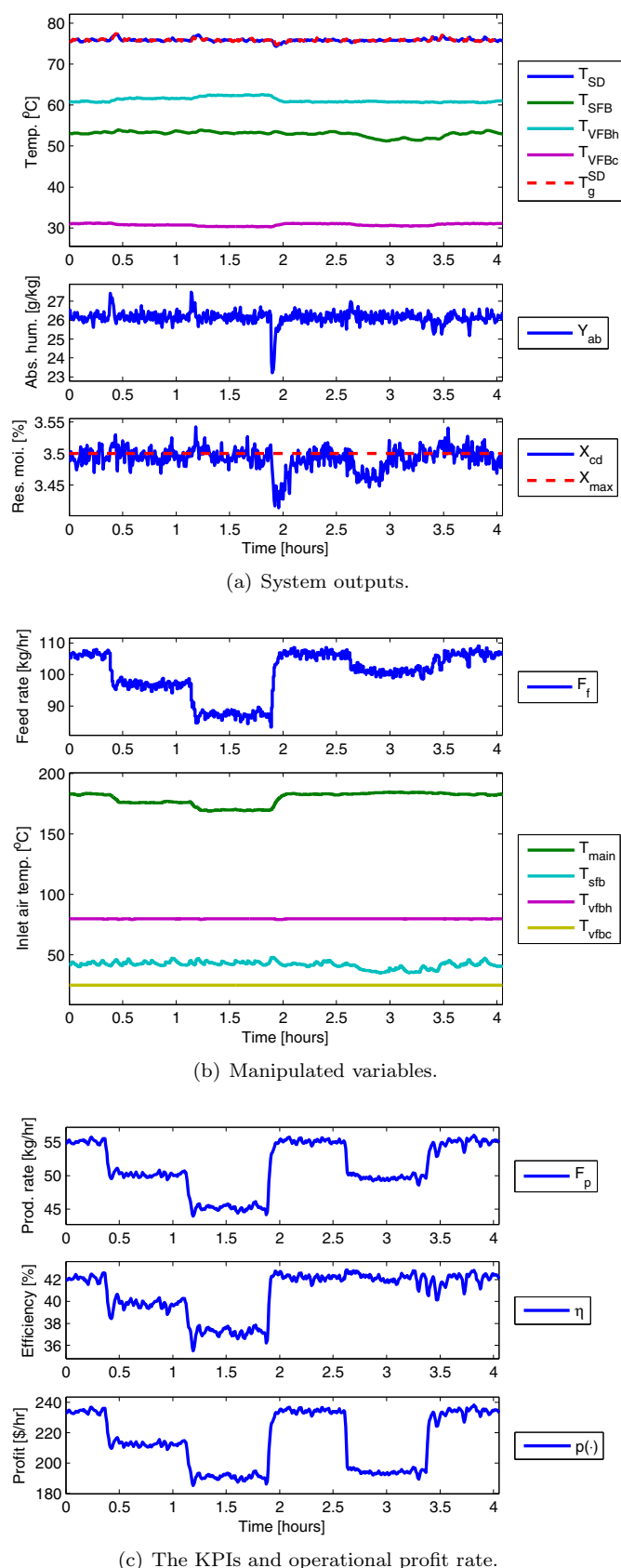


Fig. 4. E-NMPC seeking to maximize profit for the disturbance scenario given in Fig. 2. Red lines indicate constraints.